Philosophical Magazine
Vol. 88, Nos. 18–20, 21 June–11 July 2008, 2615–2626

Ab-initio theory of temperature-dependent magneto-resistivities

Á. Buruzs[a]*, L. Szunyogh[ab] and P. Weinberger[c]

[a]*Center for Computational Materials Science, Technical University Vienna, A-1060 Wien, Gumpendorfer Strasse 1a;* [b]*Department of Theoretical Physics, Budapest University of Technology and Economics, Budafoki u. 8., H-1111Budapest, Hungary;* [c]*Center for Computational Nanoscience, A-1010 Wien, Seilerstätte 10/22*

(*Received 28 May 2008; final version received 19 August 2008*)

We present the first *ab-initio* type descriptions of the temperature dependence of the magnetic part of the electrical conductivity. We implemented the Disordered Local Moment (DLM) scheme into Kubo's linear-response formalism using the screened Korringa-Kohn-Rostoker (KKR) approach. In order to test the proposed scheme, we calculated the magnetic resistivity of bulk Fe and Co. The results seem to give a qualitatively correct temperature dependence of the magnetic part of the electrical resistivity in the ferromagnetic region.

Keywords: theory of electronic transport; electronic conduction in metals; spin-disorder scattering

1. Introduction

The age of spintronics started with the discovery of giant magnetoresistance (GMR) in 1988 [1,2]. Presently GMR based magnetic read heads are commonly used in magnetic recording [3]. The understanding of the underlying effects as well as the design of new spintronics devices require a proper theoretical description of magneto-resistivities. Nowadays zero-temperature *ab-initio* descriptions of the electric resistivity have become almost a standard procedure by making use of the Kubo-Greenwood equation and the Screened Korringa-Kohn-Rostoker method [4–6]. At non-zero temperatures, however, additional effects such as electron–phonon scattering and electron–magnon scattering become rather important. Assuming that the electron–phonon interaction ($R_{\mathrm{e-ph}}$), impurity scattering (R_{i}) and the magnetic part (R_{M}) contribute additively, the total temperature-dependent resistances of the parallel (P) and the antiparallel (AP) configurations of a spin valve corresponding to a simple parent lattice are given by

$$R^{P(\mathrm{AP})}(T) = R_{\mathrm{M}}^{P(\mathrm{AP})}(T) + R_{\mathrm{i}} + R_{\mathrm{e-ph}}(T), \tag{1}$$

where the impurity and phonon scattering contributions are clearly independent of the magnetic configuration. The temperature-dependent GMR ratio,

$$\mathrm{GMR}(T) = \frac{R^{\mathrm{AP}} - R^{P}}{R^{P}} = \frac{R_{\mathrm{M}}^{\mathrm{AP}}(T) - R_{\mathrm{M}}^{P}(T)}{R_{\mathrm{M}}^{P}(T) + R_{\mathrm{i}} + R_{\mathrm{e-ph}}(T)}, \tag{2}$$

*Corresponding author. Email: ab@cms.tuwien.ac.at

ISSN 1478–6435 print/ISSN 1478–6443 online

DOI: 10.1080/14786430802438200
http://www.informaworld.com

depends therefore only in the denominator on the temperature-dependent phonon–electron contribution.

Calculations of the GMR ratio at zero temperature with the *ab-initio* Kubo–KKR method were performed for example by Weinberger and Szunyogh for a FeCo spin valve structure [7]. Clearly enough an *ab-initio* evaluation of temperature-dependent GMR ratios would also require a proper description of the temperature dependence of the magnetic resistivity. Earlier theoretical studies dealing with the problem of temperature-dependent magnetic resistivities, $\varrho_{\mathrm{M}}(T)$, started either from the Boltzmann equation using a simple s-d scattering model Hamiltonian [8–10], or applying the so-called two-current model of Fert [11–15]. In both cases experimental parameters were used in order to determine $\varrho_{\mathrm{M}}(T)$. According to our knowledge up-to-now there is no fully *ab-initio* description for the temperature-dependent magneto-resistivity in the literature. The aim of this paper is therefore to develop a theoretical tool for the calculation of $\varrho_{\mathrm{M}}(T)$. For this purpose we implemented the Disordered Local Moment (DLM) scheme in the KKR-Kubo formalism. As a trial system we tested this new approach for the bulk systems Fe and Co. Quite clearly the present formalism can easily be carried over to alloyed layered systems (two-dimensional translational symmetry) by making use of the properties of the screened-KKR method [16]. Only then does an evaluation of the GMR(T) of a given system become accessible.

2. Theory

2.1. *The Disordered Local Moment approach*

The Disordered Local Moments (DLM) theory in the context of the Korringa-Kohn-Rostoker Coherent Potential Approximation (KKR–CPA) was proposed originally by Györffy et al. [17] and is based on the idea that in itinerant metallic magnets, on a certain time-scale τ, which is small compared to the characteristic time of spin fluctuations, but longer than the electron hopping times, the spin orientations of the electrons leaving an atomic site are sufficiently correlated with those arriving such that a nonzero magnetization exists when the appropriate quantity is averaged over τ. In the DLM scheme the magnetic excitations are modelled by associating local spin-polarization axes $\{\hat{e}\}$ with all lattice sites that vary very slowly on the time-scale of the electronic motions. These local moment degrees of freedom produce local magnetic fields centred at lattice sites which in turn affect the electronic motions and are self-consistently maintained by them. By taking appropriate ensemble averages over orientational configurations the system's magnetic properties can be determined. As a mean field approximation, the CPA was applied for these ensemble averages.

The DLM for three-dimensional translationally invariant systems was first used to calculate the magnetic properties of the paramagnetic state of ferromagnetic materials [17,18], and later on was generalized to non-zero temperature ferromagnetic states by taking into account relativistic effects in order to evaluate temperature-dependent magnetic anisotropies [19,20]. An implementation of the DLM in the screened-KKR method [16]; i.e. an implementation for two-dimensional translationally invariant systems facilitated the description of anisostropic surface magnetism and thin films [21]. In the following section we present an implementation of this particular DLM scheme into the KKR-Kubo-Greenwood formalism.

2.2. *The Kubo-Greenwood equation at finite temperatures*

For the electrical conductivity calculations we used Kubo's [22] linear-response theory. In this approximation the static ($\boldsymbol{q}=0, \omega=0$) electrical conductivity is given by [23]:

$$\sigma_{\mu\mu} = \frac{\pi\hbar}{NV_{\mathrm{at}}}\left\langle \sum_{m,n} J^{\mu}_{\mathrm{mn}} J^{\mu}_{\mathrm{nm}} \delta(\varepsilon_{\mathrm{F}} - \varepsilon_m)\delta(\varepsilon_{\mathrm{F}} - \varepsilon_n)\right\rangle, \tag{3}$$

where $\mu = \{x, y, z\}$, N is the number of atoms, V_{at} the atomic volume, $\langle \ldots \rangle$ refers to the statistical average, ε_{F} is the Fermi energy, and J^{μ}_{mn} are the matrix elements of the current operator,

$$J^{\mu}_{\mathrm{mn}} = \langle m|J^{\mu}|n\rangle,$$

in the basis of the eigenstates $|n\rangle$ of the unperturbed Hamiltonian, the current operator being given by

$$\vec{J}(\boldsymbol{r}) = \mathrm{ec}\psi^{+}(\boldsymbol{r})\overrightarrow{\alpha}\,\psi(\boldsymbol{r}). \tag{4}$$

By making use of the identity,

$$\sum_n |n\rangle\langle n|\delta(\varepsilon - \varepsilon_n) = -\frac{1}{\pi}\mathrm{Im}\mathrm{G}^{+}(\varepsilon) = -\frac{1}{2\pi i}[G^{+}(\varepsilon) - G^{-}(\varepsilon)], \tag{5}$$

$$G^{\pm}(\varepsilon) = \lim_{\eta\to\pm 0} G(\varepsilon + i\eta)(\varepsilon). \tag{6}$$

Equation (3) can be rewritten as

$$\sigma_{\mu\mu} = \frac{\pi\hbar}{NV_{\mathrm{at}}}\mathrm{Tr}\left\langle J^{\mu}\mathrm{Im}\mathrm{G}^{+}(\varepsilon_{\mathrm{F}})J^{\mu}\mathrm{Im}\mathrm{G}^{+}(\varepsilon_{\mathrm{F}})\right\rangle, \tag{7}$$

or, by introducing the notation

$$\varepsilon^{\pm} = \lim_{\eta\to\pm 0} \varepsilon + i\eta,$$

as

$$\sigma_{\mu\mu} = \frac{1}{4}\left\{\tilde{\sigma}_{\mu\mu}(\varepsilon^{+}, \varepsilon^{+}) + \tilde{\sigma}_{\mu\mu}(\varepsilon^{-}, \varepsilon^{-}) - \tilde{\sigma}_{\mu\mu}(\varepsilon^{+}, \varepsilon^{-}) - \tilde{\sigma}_{\mu\mu}(\varepsilon^{-}, \varepsilon^{+})\right\}, \tag{8}$$

where

$$\tilde{\sigma}_{\mu\mu}(\varepsilon_1, \varepsilon_2) = \frac{\pi\hbar}{NV_{\mathrm{at}}}\mathrm{Tr}\left\langle J^{\mu}\mathrm{Im}\mathrm{G}^{+}(\varepsilon_1)J^{\mu}\mathrm{Im}\mathrm{G}^{+}(\varepsilon_2)\right\rangle, \tag{9}$$

$$(\varepsilon_{\mathrm{i}} \in \{\varepsilon^{+}, \varepsilon^{-}\}; i = 1, 2). \tag{10}$$

Expressing the Green's functions in terms of scattering path operators (SPO) $\tau^{pi,qj}(\varepsilon)$ as described in [5] the resistivity can then be obtained by assuming a region consisting of n intermediate atomic layers in between two semi-infinite systems. If n tends to infinity,

the resistivity converges to the corresponding bulk value. According to [5] or [6] a typical contribution $\tilde{\sigma}_{\mu\mu}(\varepsilon_1, \varepsilon_2)$ is then given by

$$\tilde{\sigma}_{\mu\mu}(\varepsilon_1, \varepsilon_2) = \frac{\pi\hbar}{nN_0V_{\mathrm{at}}} \sum_{p=1}^{n} \sum_{i\in I(L_2)} \sum_{q=1}^{n} \sum_{j\in I(L_2)} \mathrm{Tr}\left\langle \underline{J}_{\mu}^{pi}(\varepsilon_2, \varepsilon_1)\underline{\tau}^{pi,qj}(\varepsilon_1)\underline{J}_{\mu}^{qj}(\varepsilon_1, \varepsilon_2)\underline{\tau}^{qj,pi}(\varepsilon_2)\right\rangle, \tag{11}$$

where the summations over i and j cover all pairs of sites situated in layers $0<p,\ q\leq n$. In Equation (11), N_0 is the number of atoms in a layer and $I(L_2)$ is the set of indices belonging to a simple two-dimensional lattice L_2.

In the basis of regular scattering solutions $Z_{\Lambda}^{pi}(\boldsymbol{r}_{pi}, \varepsilon)$ [24] the matrix elements of the current operator, Equation (4), are given by

$$J_{\mu,\Lambda\Lambda'}^{pi}(\varepsilon_1, \varepsilon_2) = \mathrm{ec}\int_{\mathrm{WS}} Z_{\Lambda}^{pi}(\boldsymbol{r}_{pi}, \varepsilon_1)^{+}\alpha_{\mu}Z_{\Lambda'}^{pi}(\boldsymbol{r}_{pi}, \varepsilon_2)d^3\boldsymbol{r}_{pi}, \tag{12}$$

where $\Lambda=\kappa\mu$ and the integration has to be performed over a particular unit (Wigner-Seitz) cell. Provided that two-dimensional invariance applies in all layers under consideration we can make use of the fact that

$$J_{\mu}^{p}(\varepsilon_1, \varepsilon_2) = J_{\mu}^{p0}(\varepsilon_1, \varepsilon_2) = J_{\mu}^{pi}(\varepsilon_1, \varepsilon_2)\forall i \in I(L_2). \tag{13}$$

For this very reason one can easily see that for each layer p the sum over $i\in I(L_2)$ gives N_0 times the same contribution, therefore,

$$\tilde{\sigma}_{\mu\mu}(\varepsilon_1, \varepsilon_2) = \frac{C}{n}\sum_{p=1}^{n}\sum_{q=1}^{n}\left(\sum_{j\in I(L_2)} \mathrm{Tr}\left\langle \underline{J}_{\mu}^{p}(\varepsilon_2, \varepsilon_1)\underline{\tau}^{p0,qj}(\varepsilon_1)\underline{J}_{\mu}^{q}(\varepsilon_1, \varepsilon_2)\underline{\tau}^{qj,p0}(\varepsilon_2)\right\rangle\right), \tag{14}$$

with $C=\pi\hbar/V_{\mathrm{at}}$. If we neglect the so-called vertex corrections [4] we can reformulate the statistical average of the products in the above equation as

$$\begin{aligned}\tilde{\sigma}_{\mu\mu}(\varepsilon_1, \varepsilon_2) = \frac{C}{n}\sum_{p=1}^{n}\sum_{q=1}^{n}\sum_{j\in I(L_2)}\int\int \mathrm{d}\hat{e}_0\,\mathrm{d}\hat{e}_j P(\{\hat{e}_0, \hat{e}_j\}) \\ \times \mathrm{Tr}\left(\underline{J}_{\mu}^{p0}(\varepsilon_2, \varepsilon_1, \hat{e}_0)\left\langle\underline{\tau}^{p0,qj}(\varepsilon_1)\right\rangle_{p0\hat{e}_0,\,qj\hat{e}_j}\underline{J}_{\mu}^{qj}(\varepsilon_1, \varepsilon_2, \hat{e}_j)\left\langle\underline{\tau}^{qj,p0}(\varepsilon_2)\right\rangle_{qj\hat{e}_j,\,p0\hat{e}_0}\right)\end{aligned} \tag{15}$$

where $P(\{\hat{e}_0, \hat{e}_j\})$ is the probability of an $\{\hat{e}_0, \hat{e}_j\}$ configuration. The restricted averages $\langle\tau^{p0,qj}(\varepsilon_1)\rangle_{p0\hat{e}_0,qj\hat{e}j}$ can be obtained by freezing in the local moment directions in sites 0 and j and averaging over all other lattice sites. Note that now also the current matrix elements are direction dependent, since a rotational transformation of Equation (12) yields

$$J_{\mu,\Lambda\Lambda'}^{p}(\varepsilon_1, \varepsilon_2, \hat{e}) = \sum_{\nu=1}^{3}\sum_{\Gamma\,\Gamma'} O_{\Lambda\Gamma}^{*}R_{\mu\nu}J_{\nu,\Gamma:\Gamma'}^{p}(\varepsilon_1, \varepsilon_2)O_{\Gamma'\Lambda'}, \tag{16}$$

where $J_{\mu,\Gamma:\Gamma'}^{p}(\varepsilon_1, \varepsilon_2)$ refers to a current matrix if the local moment points along the $\hat{z}$ axis, and $O_{\Lambda\Gamma}$ and $R_{\mu\nu}$ denote appropriate representations of that rotation which takes the $\hat{z}$ axis into the $\hat{e}$ axis in the angular momentum as well as in coordinate space, respectively.

The sum in Equation (15) can be split into a site-diagonal and an off-diagonal term,

$$\tilde{\sigma}_{\mu\mu}(\varepsilon_1, \varepsilon_2) = \tilde{\sigma}_{\mu\mu}^{0}(\varepsilon_1, \varepsilon_2) + \tilde{\sigma}_{\mu\mu}^{1}(\varepsilon_1, \varepsilon_2), \tag{17}$$

where the diagonal part is given by

$$\tilde{\sigma}^0_{\mu\mu}(\varepsilon_1,\varepsilon_2)=\frac{C}{n}\sum_{p=1}^{n}\int \mathrm{d}\hat{e}P_p(\hat{e})\mathrm{Tr}\Big(\underline{J}^p_\mu(\varepsilon_2,\varepsilon_1,\hat{e})\big\langle\underline{\tau}^{p0,p0}(\varepsilon_1)\big\rangle_{p0\,\hat{e}}\,\underline{J}^p_\mu(\varepsilon_1,\varepsilon_2,\hat{e})\big\langle\underline{\tau}^{p0,p0}(\varepsilon_2)\big\rangle_{p0\,\hat{e}}\Big). \quad (18)$$

Expressing the restricted scattering path operators within the single-site CPA approximation [24] and using the underlying two-dimensional translational invariance,

$$\big\langle\underline{\tau}^{pi,pi}(\varepsilon)\big\rangle_{pi\hat{e}}=\underline{\tau}^{pi,pi}_c(\varepsilon)\underline{D}^{pi}(\varepsilon,\hat{e})=\underline{\tau}^{pp}_c(\varepsilon)\underline{D}^{p}(\varepsilon,\hat{e})\forall i\in I(L_2), \quad (19)$$

one obtains

$$\tilde{\sigma}^0_{\mu\mu}(\varepsilon_1,\varepsilon_2)=\frac{C}{n}\sum_{p=1}^{n}\int \mathrm{d}\hat{e}P_p(\hat{e})\mathrm{Tr}\Big[\underline{J}^p_\mu(\varepsilon_2,\varepsilon_1,\hat{e})\underline{\tau}^{pp}_c(\varepsilon_1)\underline{D}^{p}(\varepsilon_1,\hat{e})\underline{J}^p_\mu(\varepsilon_1,\varepsilon_2,\hat{e})\underline{\tau}^{pp}_c(\varepsilon_2)\underline{D}^{p}(\varepsilon_2,\hat{e})\Big], \quad (20)$$

where $P_p(\hat{e})$ is the probability density function of the local moment direction distribution in layer p [21], and

$$\underline{D}^{p}(\varepsilon,\hat{e})=[I+(\underline{m}_p(\varepsilon,\hat{e})-\underline{m}_{c,p}(\varepsilon_1))\underline{\tau}^{pp}_c(\varepsilon)]^{-1},$$

with $\underline{m}_{c,p}(\varepsilon_1)$ and $\underline{m}_p(\varepsilon,\hat{e})$ being the inverse scattering matrices [24] of the coherent media, and the local moment 'impurity' pointing in the $\hat{e}$ direction, respectively.

The site off-diagonal part can be further decomposed into two terms:

$$\tilde{\sigma}^1_{\mu\mu}(\varepsilon_1,\varepsilon_2)=\tilde{\sigma}^2_{\mu\mu}(\varepsilon_1,\varepsilon_2)+\tilde{\sigma}^3_{\mu\mu}(\varepsilon_1,\varepsilon_2), \quad (21)$$

where

$$\tilde{\sigma}^2_{\mu\mu}(\varepsilon_1,\varepsilon_2)=\frac{C}{n}\sum_{p=1}^{n}\sum_{q=1}^{n}(1-\delta_{pq})\sum_{j\in I(L_2)}\mathrm{Tr}\Big\langle\underline{J}^p_\mu(\varepsilon_2,\varepsilon_1)\underline{\tau}^{p0,qj}(\varepsilon_1)\underline{J}^q_\mu(\varepsilon_1,\varepsilon_2)\underline{\tau}^{qj,p0}(\varepsilon_2)\Big\rangle \quad (22)$$

and

$$\tilde{\sigma}^3_{\mu\mu}(\varepsilon_1,\varepsilon_2)=\frac{C}{n}\sum_{p=1}^{n}\sum_{j\in I(L_2)\setminus\{0\}}\mathrm{Tr}\Big\langle\underline{J}^p_\mu(\varepsilon_2,\varepsilon_1)\underline{\tau}^{p0,pj}(\varepsilon_1)\underline{J}^p_\mu(\varepsilon_1,\varepsilon_2)\underline{\tau}^{pj,p0}(\varepsilon_2)\Big\rangle. \quad (23)$$

As one can see $\tilde{\sigma}^2_{\mu\mu}$ arises from sites located in different layers, while $\tilde{\sigma}^3_{\mu\mu}$ arises from sites in one and the same layer. Restricting the local moments on two different sites, the restricted SPO can be written as [24]

$$\big\langle\underline{\tau}^{p0,qj}(\varepsilon)\big\rangle_{p0\hat{e}_i,\,qj\hat{e}_j}=\underline{\tilde{D}}^{p}(\varepsilon,\hat{e}_i)\underline{\tau}^{p0,qj}_c(\varepsilon)\underline{D}^{q}(\varepsilon,\hat{e}_j),$$

with

$$\underline{\tilde{D}}^{p}(\varepsilon,\hat{e})=[I+\underline{\tau}^{pp}_c(\varepsilon)(\underline{m}_p(\varepsilon,\hat{e})-\underline{m}_{c,p}(\varepsilon))]^{-1}.$$

Using this expression and neglecting vertex corrections $\tilde{\sigma}^2_{\mu\mu}$ can be written as

$$\tilde{\sigma}^2_{\mu\mu}(\varepsilon_1,\varepsilon_2) = \frac{C}{n}\sum_{p=1}^{n}\sum_{q=1}^{n}(1-\delta_{pq})\sum_{j\in I(L_2)}\int\int \mathrm{d}\hat{e}_{\mathrm{i}}\,\mathrm{d}\hat{e}_j P_p(\hat{e}_{\mathrm{i}})P_q(\hat{e}_j) \times \mathrm{Tr}\Big\{\underline{J}^p_\mu(\varepsilon_2,\varepsilon_1,\hat{e}_{\mathrm{i}})\underline{\tilde{D}}^p(\varepsilon_1,\hat{e}_{\mathrm{i}})\underline{\tau}_c^{p0,qj}(\varepsilon_1)\underline{D}^q(\varepsilon_1,\hat{e}_j) \times \underline{J}^q_\mu(\varepsilon_1,\varepsilon_2)\underline{\tilde{D}}^q(\varepsilon_2,\hat{e}_j)\underline{\tau}_c^{qj,p0}(\varepsilon_2)\underline{D}^p(\varepsilon_2,\hat{e}_{\mathrm{i}})\Big\},$$

or, by introducing the quantity,

$$\underline{\tilde{J}}^{p,\mathrm{av}}_\mu(\varepsilon_2,\varepsilon_1) = \int \mathrm{d}\hat{e}P_p(\hat{e}_{\mathrm{i}})\underline{D}^p(\varepsilon_2,\hat{e})\underline{J}^p_\mu(\varepsilon_2,\varepsilon_1,\hat{e})\underline{\tilde{D}}^p(\varepsilon_1,\hat{e}), \tag{24}$$

as

$$\tilde{\sigma}^2_{\mu\mu}(\varepsilon_1,\varepsilon_2) = \frac{C}{n}\sum_{p=1}^{n}\sum_{q=1}^{n}(1-\delta_{pq}) \times \sum_{j\in I(L_2)}\mathrm{Tr}\Big\{\underline{\tilde{J}}^{p,\mathrm{av}}_\mu(\varepsilon_2,\varepsilon_1)\underline{\tau}_c^{p0,qj}(\varepsilon_1)\underline{\tilde{J}}^{q,\mathrm{av}}_\mu(\varepsilon_1,\varepsilon_2)\underline{\tau}_c^{qj,p0}(\varepsilon_2)\Big\}.$$

From the Fourier transformed form,

$$\underline{\tau}_c^{p0,qj}(\varepsilon) = \frac{1}{\Omega_{\mathrm{SBZ}}}\int e^{i\vec{k}\cdot\vec{R}_j}\underline{\tau}_c^{pq}(\vec{k},\varepsilon)d^2k,$$

where Ω_{SBZ} is the volume of the surface Brillouin zone, and using the orthogonality relations,

$$\sum_{j\in I(L_2)}\underline{\tau}_c^{p0,qj}(\varepsilon_1)\underline{\tau}_c^{qj,p0}(\varepsilon_2) = \frac{1}{\Omega_{\mathrm{SBZ}}}\int \underline{\tau}_c^{pq}(\vec{k},\varepsilon_1)\underline{\tau}_c^{qp}(\vec{k},\varepsilon_2)d^2k,$$

we finally obtain for $\tilde{\sigma}^2_{\mu\mu}$,

$$\tilde{\sigma}^2_{\mu\mu}(\varepsilon_1,\varepsilon_2) = \frac{C}{n\Omega_{\mathrm{SBZ}}}\sum_{p=1}^{n}\sum_{q=1}^{n}(1-\delta_{pq})\int \mathrm{Tr}\Big\{\underline{\tilde{J}}^{p,\mathrm{av}}_\mu(\varepsilon_2,\varepsilon_1)\underline{\tau}_c^{pq}(\vec{k},\varepsilon_1)\underline{\tilde{J}}^{q,\mathrm{av}}_\mu(\varepsilon_1,\varepsilon_2)\underline{\tau}_c^{qp}(\vec{k},\varepsilon_2)\Big\}d^2k. \tag{25}$$

Similarly, using again a lattice Fourier transformation we obtain for $\tilde{\sigma}^3_{\mu\mu}(\varepsilon_1,\varepsilon_2)$,

$$\tilde{\sigma}^3_{\mu\mu}(\varepsilon_1,\varepsilon_2) = \frac{C}{n\Omega_{\mathrm{SBZ}}}\sum_{p=1}^{n}\int \mathrm{Tr}\Big\{\underline{\tilde{J}}^{p,\mathrm{av}}_\mu(\varepsilon_2,\varepsilon_1)\underline{\tau}_c^{pp}(\vec{k},\varepsilon_1)\underline{\tilde{J}}^{p,\mathrm{av}}_\mu(\varepsilon_1,\varepsilon_2)\underline{\tau}_c^{pp}(\vec{k},\varepsilon_2)\Big\}d^2k + \tilde{\sigma}^{3\mathrm{corr}}_{\mu\mu}(\varepsilon_1,\varepsilon_2), \tag{26}$$

where $\tilde{\sigma}^{3\mathrm{corr}}_{\mu\mu}(\varepsilon_1,\varepsilon_2)$ arises from extending the sum in Equation (24) to $\forall j\in I(L_2)$ and subtracting the term for $j=0$,

$$\begin{aligned}\tilde{\sigma}^{3\mathrm{corr}}_{\mu\mu}(\varepsilon_1,\varepsilon_2) &= -\frac{C}{n}\sum_{p=1}^{n}\int\int \mathrm{d}\hat{e}_{\mathrm{i}}\,\mathrm{d}\hat{e}_j P_p(\hat{e}_{\mathrm{i}})P_p(\hat{e}_j) \times \mathrm{Tr}\Big\{\underline{J}^p_\mu(\varepsilon_2,\varepsilon_1,\hat{e}_{\mathrm{i}})\underline{\tilde{D}}^p(\varepsilon_1,\hat{e}_{\mathrm{i}})\underline{\tau}_c^{pp}(\varepsilon_1)\underline{D}^p(\varepsilon_1,\hat{e}_j) \\ &\quad \times \underline{J}^p_\mu(\varepsilon_1,\varepsilon_2)\underline{\tilde{D}}^p(\varepsilon_2,\hat{e}_j)\underline{\tau}_c^{pp}(\varepsilon_2)\underline{D}^p(\varepsilon_2,\hat{e}_{\mathrm{i}})\Big\} \\ &= -\frac{C}{n}\sum_{p=1}^{n}\mathrm{Tr}\Big\{\underline{\tilde{J}}^{p,\mathrm{av}}_\mu(\varepsilon_2,\varepsilon_1)\underline{\tau}_c^{pp}(\varepsilon_1)\underline{\tilde{J}}^{p,\mathrm{av}}_\mu(\varepsilon_1,\varepsilon_2)\underline{\tau}_c^{pp}(\varepsilon_2)\Big\}.\end{aligned}$$

Summarizing all the terms, the electrical conductivity obtained from Equation (8) is of the form,

$$\tilde{\sigma}_{\mu\mu}(\varepsilon_1,\varepsilon_2) = \frac{C}{n}\sum_{p=1}^{n}\Bigg\{\int P_p(\hat{e})\mathrm{Tr}\Big\{\underline{J}_{\mu}^{p0}(\varepsilon_2,\varepsilon_1,\hat{e})\underline{\tau}_c^{pp}(\varepsilon_1)\underline{D}^{p}(\varepsilon_1,\hat{e})\underline{J}_{\mu}^{p}(\varepsilon_1,\varepsilon_2,\hat{e})\underline{\tau}_c^{pp}(\varepsilon_2)\underline{D}^{p}(\varepsilon_2,\hat{e})\Big\}\,\mathrm{d}\hat{e}$$
$$-\mathrm{Tr}\Big(\underline{\tilde{J}}_{\mu}^{p,\mathrm{av}}(\varepsilon_2,\varepsilon_1)\underline{\tau}_c^{pp}(\varepsilon_1)\underline{\tilde{J}}_{\mu}^{p,\mathrm{av}}(\varepsilon_1,\varepsilon_2)\underline{\tau}_c^{pp}(\varepsilon_2)\Big)$$
$$+\frac{1}{\Omega_{\mathrm{SBZ}}}\sum_{q=1}^{n}\int\mathrm{Tr}\Big\{\underline{\tilde{J}}_{\mu}^{p,\mathrm{av}}(\varepsilon_2,\varepsilon_1)\underline{\tau}_c^{pq}(\vec{k},\varepsilon_1)\underline{\tilde{J}}_{\mu}^{q,\mathrm{av}}(\varepsilon_1,\varepsilon_2)\underline{\tau}_c^{qp}(\vec{k},\varepsilon_2)\Big\}d^2k\Bigg\}. \tag{27}$$

2.3. *Computational details*

In order to perform the calculations we first have to calculate the temperature-dependent Weiss fields as described in [21], which provide the probability distributions $P_p(\hat{e})$, and then evaluate Equation (27).

We calculated the magnetic part of the conductivity of bulk Fe and Co using Equations (27) and (8) in terms of the screened KKR. For the $\vec{k}$ integration in Equation (27) we used a quadrature with 1600 points in the two-dimensional Brillouin zone, which gave converged results. The so-called intermediate region consists of n atomic layers; the $\tilde{\sigma}(\varepsilon_F \pm i\delta, \varepsilon_F \pm i\delta)$ in Equation (8) were calculated for finite imaginary parts δ of the Fermi energy. A side-effect of considering a finite number of atomic layers is a $(1/n)$-like decay [25] in the calculated resistivity

$$\varrho_{\mu\mu}(n,\delta) = \frac{1}{\sigma_{\mu\mu}(n,\delta)} \approx \varrho_{\mu\mu}(\delta) + \frac{\Delta\varrho_{\mu\mu}(\delta)}{n}. \tag{28}$$

Therefore plotting $n\varrho_{\mu\mu}(n,\delta)$ versus n the slope of the curve for large enough n yields $\varrho_{\mu\mu}(\delta)$, the bulk resistivity value at a given value of δ. In practice it turned out that $n\varrho_{\mu\mu}(n,\delta)$ is already linear in n for $n \geqslant 50$ layers. For the δ dependence of the resistivity we found the same linear dependence already described in the literature [26,27], namely

$$\varrho_{\mu\mu} = \lim_{\delta\to 0}\varrho_{\mu\mu}(\delta). \tag{29}$$

For this continuation to the real axis we used $\varrho_{\mu\mu}(\delta)$ values corresponding to $\delta = 1$ and 2 mRyd. The magnetization direction was chosen to be perpendicular to the intermediate layers, i.e., pointed along to the $\hat{z}$ direction, which in turn causes a small difference between the ϱ_{zz} and $\varrho_{xx} = \varrho_{yy}$ components of the resistivity. Since this difference turned out to be smaller than 1 $\mu\Omega$ cm in the whole temperature regime, we confine ourselves to using the ϱ_{zz} component of the resistivity only.

3. Results for bulk Fe and Co

First we calculated the temperature-dependent Weiss fields, which are needed for the finite temperature thermal averaging in Equation (27). In using the experimental lattice parameter (5.4 a.u.) we obtained a too large Curie temperature (T_c) for pure bcc Fe,

namely 1670 K, which is about 60% larger than the experimental T_c of 1040 K. This deficiency is probably due to a shortcoming of the mean-field approximation. However, for a lattice parameter of 5.07 a.u., we can recover the experimental T_c. In Figure 1 we show the calculated T_c for bcc Fe versus the lattice parameter used in the calculations. It should be noted that the lattice parameter at the experimental Curie temperature is even larger than the one at zero temperature, namely 5.55 a.u. according to Section 1.1.2.2 of [28]. Since the LDA usually yields lattice parameters smaller than the experimental ones (5.3 a.u. [29]) Györffy et al. [17] used this particular lattice parameter, and in employing the non-relativistic version of the DLM found a Curie temperature of 1250 K in terms of the divergence of the paramagnetic spin susceptibility.

As a second test system we chose Co bulk which – as is well-known – shows a phase transition from hcp to fcc at about 600–800 K, which, however, by using only the fcc geometry in the whole temperature regime was neglected in the present calculations. At zero temperature the theoretical LDA lattice parameter (6.69 a.u. [29]) differs by less than 1% from the experimental one. At the experimental T_c, however, the lattice parameter is considerably enlarged, namely amounts to 6.84 a.u. [28]. In the Co case the DLM considerably underestimates the Curie temperature; even at 6.84 a.u. we only get 950 K. The experimental T_c is 1380 K, which can be simulated in terms of the DLM by using a lattice constant of 7.04 a.u.; see also Figure 2.

From the self-consistent potentials corresponding to the paramagnetic DLM state we first calculated the Weiss fields as described in [21] for specific temperature points. In using these Weiss fields we then calculated the corresponding temperature-dependent electrical conductivities in terms of Equation (8). For low temperatures, it seems that the ferromagnetic potentials (corresponding to zero temperature, screened KKR without DLM) describe the electronic structure better. It turned out, however, that the difference between the ferromagnetic and paramagnetic potential only influences the conductivity results marginally. In Figure 3 the results for bcc Fe are displayed corresponding (a) to the experimental lattice parameter which gave an overestimated Curie temperature, and (b) for

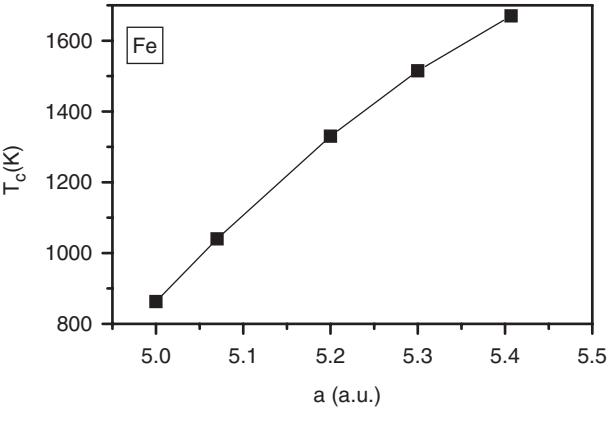

Figure 1. Calculated Curie temperature for bcc Fe corresponding to different lattice parameters. The experimental zero temperature lattice parameter is 5.4 a.u., the experimental Curie temperature is 1040 K.

the lattice parameter that recovers the experimental Curie temperature. For comparison we also show the experimental total resistivity values from [28].

It became customary [30] to assume that well above the Curie temperature only phonon–electron interactions contribute to the resistivity. By using the Bloch-Grüneisen formula [31],

$$\varrho_{\mathrm{ph}-e}(T) = K\left(\frac{T}{\Theta_{\mathrm{D}}}\right)^5 J\left(\frac{\Theta_{\mathrm{D}}}{T}\right), \tag{30}$$

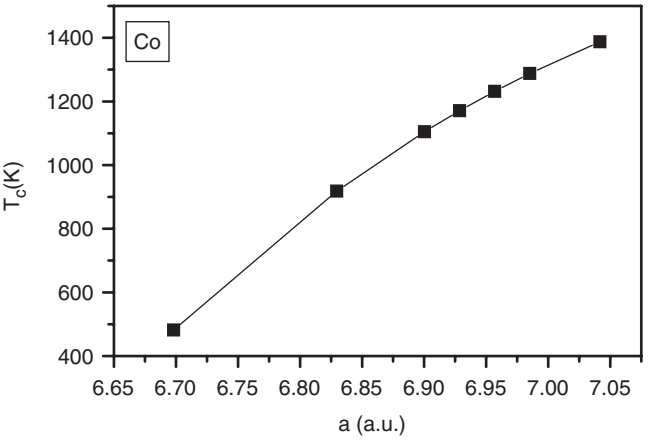

Figure 2. Calculated Curie temperature of fcc Co corresponding to different lattice parameters. The experimental Curie temperature is 1380 K, at which the lattice parameter is 6.84 a.u. [28].

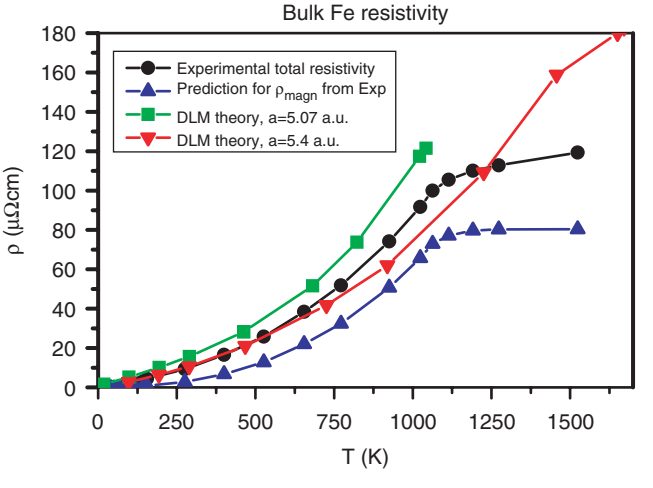

Figure 3. (Colour online) Black circles: experimental total resistivity from [28]. Blue up-triangles: magnetic part of the resistivity with detached phonon–electron contribution of Bloch-Grüneisen form. Red down triangles: our results corresponding to the experimental lattice parameter (5.4 a.u.), green squares: for a lattice constant of 5.07 a.u.

where Θ_D is the Debye temperature, and J is a Debye integral [31], we can fit the parameter K to the linear part of the experimental Fe resistivity above T_c. Subtracting this Bloch-Grüneisen term from the total resistivity we get a first guess for the magnetic resistivity, which is also displayed in Figure 3. It has to be mentioned that this approximation, although used by Weiss and Marotta [30] for several magnetic metals, is still theoretically not justified, since in this procedure the magnon–phonon interactions [8] are completely neglected.

It can be seen from this figure that the DLM gives the right order of magnitude of the magnetic resistivity, but however is systematically too large. The deviation between the calculated resistivities corresponding to the two different lattice parameters used is less than 40% at room temperature and also for temperatures far below the Curie temperature. The DLM result for the experimental lattice parameter fits well to the experimental total resistivity for temperatures below about 700 K, although the total resistivity ought to be larger than the pure magnetic contribution. We also have to mention that the DLM gives a constant magnetic resistivity in the paramagnetic phase since there the probability density function is constant, i.e., is temperature independent above the Curie temperature.

The results for fcc Co are shown in Figure 5. It can be seen that below 700 K the DLM results corresponding to different lattice parameters differ by about 30%. The common feature of the calculated curves is an up-turning just below the Curie temperature. This again seems to be a consequence of the applied mean field approximation. We can see that below 700 K the computed resistivity curves are by about 50–100% above the experimental total resistivity, which as should be recalled, contains all possible contributions. In the case of Co the above-mentioned method to subtract the phonon–electron contribution by using a fit for the Bloch-Grüneisen formula doesn't work sufficiently well, because below 600 K a negative value for the (experimental) magnetic resistivity is obtained, see Figure 4, which of course does not make any sense at all.

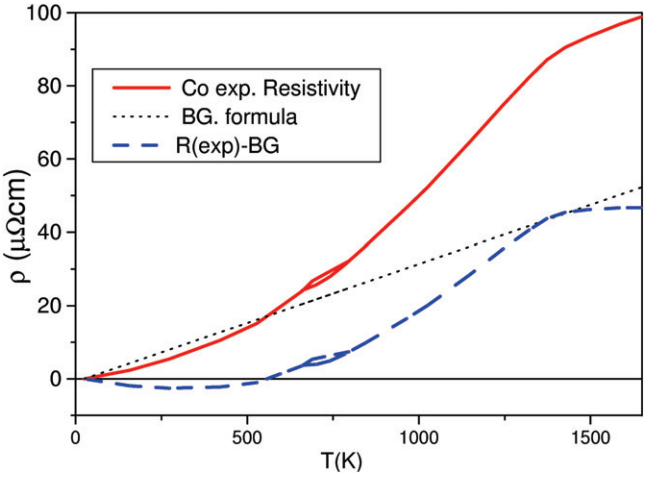

Figure 4. (Colour online) Experimental resistivity of Co (red straight curve) and of the Bloch-Grüneisen (BG) fitting function (black dotted). The difference of the experimental curve and the BG curve (blue dashed), which should be an approximation to the magnetic part of the resistivity, is negative below 500 K. (The loop around 700 K is the sign of an fcc-hcp phase transition.)

Weiss and Marotta [30], however, did use this method of subtraction to evaluate the high-temperature (saturated) magnetic resistivity of Co and cited a corresponding value of 50 μΩ cm. The main deficiency of this subtraction procedure probably is a consequence of different phonon–electron contributions in the hcp and fcc phases: from the slope of the resistivity in the paramagnetic phase with respect to temperature only conclusions for the fcc phonon–electron contribution can be gained. In addition, the temperature regime between the Curie temperature and the melting point is possibly too small to saturate a magnetic resistivity, thus making it difficult to detach a linear phonon–electron contribution. For this reason in Figure 5 only the experimental total resistivity is shown.

It is obvious that our DLM results overestimate the magnetic part of the resistivity, however, we have to stress that they are the very first parameter-free (*ab-initio*) results ever obtained for bulk Fe and Co. The deviations from experiment most likely emerge from an inaccurate determination of the Curie temperature which in turn is a consequence of the mean-field approximation, although also an inaccurate description of spin–spin correlations in a mean-field description probably adds to these deviations. It should be mentioned that in the case of chemically disordered systems more accurate descriptions can be given by taking into account for example vertex corrections [4]. From Figure 2 of [32] it can be seen that by taking into account vertex corrections the resistivity of non-magnetic Cu_c Zn_{1-c} is reduced by about a factor of 2. The resistivity is even further reduced by taking into account short-range ordering by means of a non-local CPA [33] instead of the single-site CPA used in the present paper. Based on the analogy between the 'chemical'-CPA and the 'spin-disorder'-CPA, we expect therefore that an inclusion of vertex corrections and of short-range order will also reduce our results for the temperature-dependent resistivity.

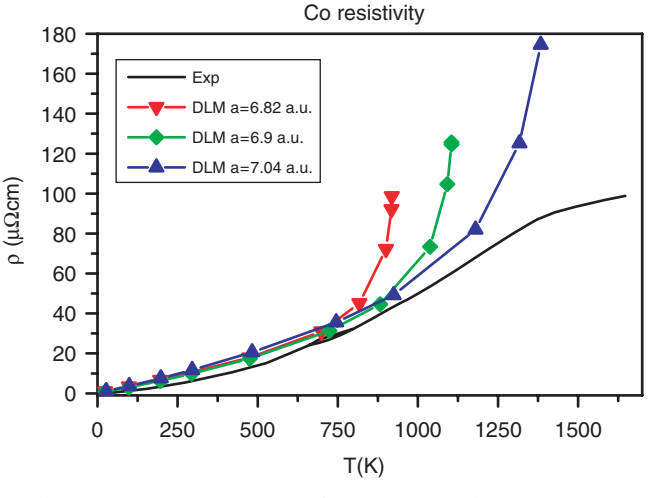

Figure 5. (Colour online) Magnetic resistivity of Co. DLM calculations corresponding to the fcc lattice parameter 6.82 a.u. (red down triangle), 6.9 a.u. (green diamond) 7.04 a.u. (blue upper triangle). The experimental [28] result is shown as a full (black) line.

References

[1] M.N. Baibich, J.M. Broto, A. Fert et al., Phys. Rev. Lett. 61 (1988) p.2472.
[2] G. Binasch, P. Grünberg, F. Saurenbach et al., Phys. Rev. B 39 (1989) p.4828.
[3] S. Wolf, A. Chtchelkanova and D. Treger, IBM J. Res. and Dev. 50 (2006) p.101.
[4] W.H. Butler, Phys. Rev. B 31 (1985) p.3206.
[5] P. Weinberger, P. Levy, J. Banhardt et al., J. Phys. Condens. Matter 8 (1996) p.7677.
[6] P. Weinberger, Phys. Rep. 377 (2003) p.281.
[7] P. Weinberger and L. Szunyogh, Phys. Rev. B 66 (2002) p.144427.
[8] D.A. Goodings, Phys. Rev. 132 (1963) p.542.
[9] B. Raquet, M. Viret, E. Sondergard et al., Phys. Rev. B 66 (2002) p.024433.
[10] B. Raquet, M. Viret, J. Broto et al., J. Appl. Phys. 91 (2002) p.8129.
[11] A. Fert and I. Campbell, Phys. Rev. Lett. 21 (1968) p.1190.
[12] A. Fert and I. Campbell, J. Phys. F: Metal Phys. 6 (1976) p.849.
[13] A. Fert, J. Phys. F: Met. Phys. 1 (1971) p.L42.
[14] A. Fert, J. Phys. C: Solid St. Phys. 2 (1969) p.1784.
[15] D.L. Mills, A. Fert and I. Campbell, Phys. Rev. B 4 (1971) p.196.
[16] L. Szunyogh, B. Ujfalussy, P. Weinberger et al., Phys. Rev. B 49 (1994) p.2721.
[17] B.L. Györffy, A.J. Pindor, J.B. Staunton et al., J. Phys. F 15 (1985) p.1337.
[18] S.S.A. Razee, J.B. Staunton, L. Szunyogh et al., Phys. Rev. B 66 (2002) p.094415.
[19] J.B. Staunton, S. Ostanin, S.S.A. Razee et al., Phys. Rev. Lett. 93 (2004) p.257204.
[20] J.B. Staunton, L. Szunyogh, Á. Buruzs et al., Phys. Rev. B 74 (2006) p.144411.
[21] Á. Buruzs, P. Weinberger, L. Szunyogh et al., Phys. Rev. B 76 (2007) p.064417.
[22] R. Kubo, J. Phys. Soc. Jpn 12 (1957) p.570.
[23] R. Kubo, Rep. Prog. Phys. 29 (1966) p.255.
[24] J. Zabloudil, R. Hammerling, L. Szunyogh et al., *Electron Scattering in Solid Matter*, *Springer Series in Solid-State Sciences*, Vol. 147, Springer, Heidelberg, 2005.
[25] C. Blaas, P. Weinberger, L. Szunyogh et al., Phys. Rev. B 60 (1999) p.492.
[26] K. Palotás, B. Lazarovits, L. Szunyogh et al., Phys. Rev. B 67 (2003) p.174404.
[27] S. Khmelevskyi, K. Palotás, L. Szunyogh et al., Phys. Rev. B 68 (2003) p.012402.
[28] M. Stearns, *Landolt–Börnstein New Series – Group III: Condensed Matter – 19A*, Springer, Berlin, 1986.
[29] M. Lezaic, P. Mavropoulos and S. Blugel, Appl. Phys. Lett. 90 (2007) p.082504.
[30] R. Weiss and A. Marotta, J. Phys. Chem. Solids. 9 (1959) p.302.
[31] J.M. Ziman, *Electrons and Phonons*, Oxford University Press, Oxford, 1960.
[32] P.R. Tulip, J.B. Staunton, S. Lowitzer et al., Phys. Rev. B 77 (2008) p.165116.
[33] D.A. Rowlands, J.B. Staunton and B.L. Györffy, Phys. Rev. B 67 (2003) p.115109.